

## POSITIONAL ISOTOPE EXCHANGE

Authors: **Frank M. Raushel**  
 Department of Chemistry  
 Texas A and M University  
 College Station, Texas

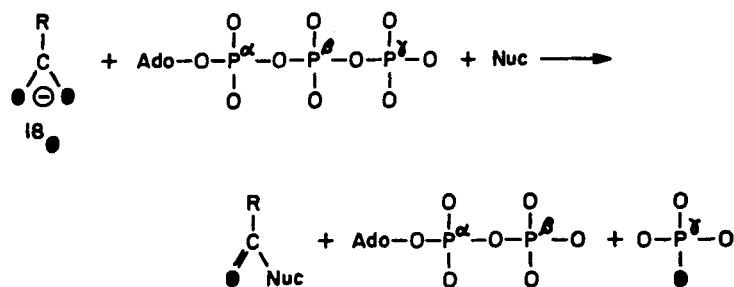
**Joseph J. Villafranca**  
 Department of Chemistry  
 Pennsylvania State University  
 University Park, Pennsylvania

Referee: **Irwin A. Rose**  
 Institute of Cancer Research  
 Fox Chase Cancer Center  
 Philadelphia, Pennsylvania

## I. INTRODUCTION

The goal of studying enzyme mechanisms is to understand the pathway taken to break existing chemical bonds and make new chemical bonds. The role of the enzyme in these transformations is to lower the activation energy barrier of the chemical step by using a combination of binding energy and covalent bond-formation between substrates or substrates and the enzyme. Thus, an understanding of enzyme catalysis requires knowledge of the nature of the enzyme-bound intermediate as well as the interaction energies among the enzyme, substrates, and enzyme-bound intermediates.

Many methods have been devised in the long history of studying enzyme catalysis to detect the chemical events throughout the conversion of substrates to products. In favorable cases enzyme-bound intermediates can be detected by spectroscopic means (UV-visible, NMR, EPR), but most often this is not the case. Thus, the largest impact has been made through the judicious use of isotopes in specific places on molecules. The "movement" of an atom from one place to another in the substrates and products usually limits the number of reasonable chemical mechanisms. In the generalized example below, the  $^{18}\text{O}$  isotope of oxygen in the carboxyl group of the substrate  $\text{RCO}_2^-$  is found in inorganic phosphate which itself is derived from the  $\gamma$ -phosphorus of ATP. Therefore, some combination of chemical steps is necessary to "move" the oxygen atom from carbon to phosphorus. Direct transfer with the formation of a C-O-P intermediate is one very likely possibility and methods to detect such a transformation are discussed throughout this article. The general phenomenon of following the movement of an isotope in a chemical reaction is termed positional isotope exchange (PIX) and this field of study was last reviewed by Rose.<sup>1</sup>



## II. QUANTITATIVE ANALYSIS OF PIX RATES

The primary utilization of the PIX technique has been to obtain evidence for enzyme-bound intermediates. For example, the existence of carboxyphosphate<sup>2,2a</sup> and  $\gamma$ -glutamyl-phosphate<sup>3</sup> in the carbamyl-phosphate synthetase and glutamine synthetase reactions mechanisms was confirmed by the observation of a PIX reaction with  $\gamma$ -<sup>18</sup>O<sub>4</sub> labeled ATP in the absence of the third substrate, NH<sub>3</sub>. However, much additional information can be obtained about the partitioning of enzyme-substrate and enzyme-product complexes by measuring the PIX rate in an enzyme-catalyzed reaction as a function of the concentration of added substrates and/or products. In favorable cases the off-rate constants, relative to  $V_{\max}$ , for all of the products and substrates from the binary and ternary complexes can be obtained with little difficulty. This methodology, therefore, complements the isotope-partitioning technique of Rose et al.,<sup>4</sup> since this information would be difficult to obtain in any other way.

PIX experiments can be designed in many ways. Quantitative PIX experiments are often conducted under conditions where all of the substrates are present (products may also be present) and the PIX rate is measured relative to the net rate of product formation. In order to measure the true partitioning of an enzyme product or enzyme-substrate complex, the product that contains the labeled groups undergoing PIX must be rapidly removed from solution once this product has been released from the surface of the protein. Otherwise, the product may dissociate from the enzyme and then reassociate and be converted back into substrate. This additional step would distort the magnitude of the observed PIX rate. The removal of the labeled product is most conveniently done by enzymatic techniques. In addition, PIX experiments can be conducted at equilibrium or under steady-state conditions and similar information can be obtained about relative rates of substrate/product interconversion.

As noted, PIX experiments are generally conducted with all of the substrates present and the PIX rate is measured relative to net product formation. Since the labeled substrate is being constantly depleted during the reaction, a correction must be made to the observed PIX rate to account for this fact. Litwin and Wimmer<sup>5</sup> have shown that the corrected rate of PIX can be obtained from the following equation

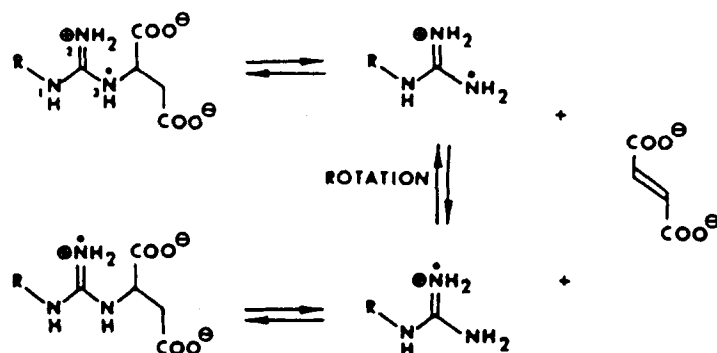
$$\frac{X}{\ln(1 - X)} \frac{A_0}{t} \ln(1 - F) \quad (1)$$

where  $A_0$  is the initial concentration of the labeled substrate,  $X$  is the fraction of substrate lost at time  $t$ , and  $F$  is the fraction of the equilibrium value for positional isotope exchange.

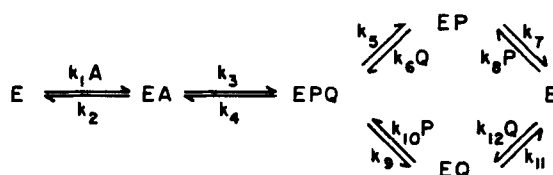
Two types of quantitative PIX experiments are possible. Either one of the products may be added to the reaction mixture in an attempt to enhance the rate of the PIX reaction relative to the net chemical rate, or the unlabeled substrate may be varied in an attempt to reduce the rate of the PIX reaction relative to the net rate of substrate turnover. These two types of experiments are discussed below.

### A. PIX Enhancement

To date there have been only two attempts to measure the effect of added products on the PIX rates. Raushel and Garrard<sup>6</sup> examined the effect of added fumarate on the positional exchange of <sup>15</sup>N and <sup>14</sup>N within argininosuccinate in the reaction catalyzed by argininosuccinate lyase. More recently, Kenyon and Reddick<sup>7</sup> have attempted to measure the PIX reactions catalyzed by creatine kinase with <sup>15</sup>N-labeled creatine. The PIX reaction catalyzed by argininosuccinate lyase is illustrated in Scheme I.



This enzyme cleaves argininosuccinate to arginine and fumarate. Specifically  $^{15}\text{N}$ -labeled argininosuccinate was enzymatically synthesized and incubated with enzyme to form enzyme-bound arginine and fumarate. If the guanidino moiety can rotate about the C-N bond then the partitioning of the enzyme-arginine-fumarate complex can be determined from the amount of scrambling of the  $^{15}\text{N}$ -label within argininosuccinate relative to the amount of arginine and/or fumarate produced in solution. A simple model of this reaction mechanism is illustrated in Scheme II.



where E, A, P, and Q represent enzyme, argininosuccinate, fumarate, and arginine, respectively. In the following analysis the rate constants  $k_6$  and  $k_{12}$  can be ignored since an excess of arginase was added to rapidly convert arginine to urea and ornithine. The ratio of the PIX rate relative to the chemical rate is determined by the partitioning of the complex EPQ. Raushel and Garrard<sup>6</sup> have shown that the ratio of the exchange rate relative to the chemical rate,  $k_r/k_f$ , is determined by the following expression for a random mechanism.

$$\frac{k_r}{k_f} = \frac{k_2 k_4 / (k_2 + k_3)}{k_5 + k_9 k_{11} / (k_{11} + k_{10}[P])} \quad (2)$$

Therefore, the ratio of  $k_r$  and  $k_f$  is determined by the amount of fumarate, [P], that is added to the reaction solution. The form of this equation as a function of [P] is illustrated in Figure 1. The intercept on the vertical axis at [P] = 0 is

$$k_r/k_f = [k_2 k_4 / (k_2 + k_3)] / (k_5 + k_9) \quad (3)$$

while the asymptote at [P] =  $\infty$  is equal to  $[k_2 k_4 / (k_2 + k_3)] / k_5$ . The ratio increases because the added [P] prevents any flux through the lower pathway. Comparison of the PIX ratio at zero and saturating fumarate thus determines the ratio of  $k_5$  and  $k_9$ .

If the release of products is ordered then Equation 2 is simplified. If fumarate is required to be released first (i.e.,  $k_5 = 0$ ) then the ratio of  $k_r$  and  $k_f$  would be linearly dependent on the concentration of added [P]. The intercept at [P] = 0 is

$$k_r/k_f = [k_2 k_4 / (k_2 + k_3)] / k_9 \quad (4)$$

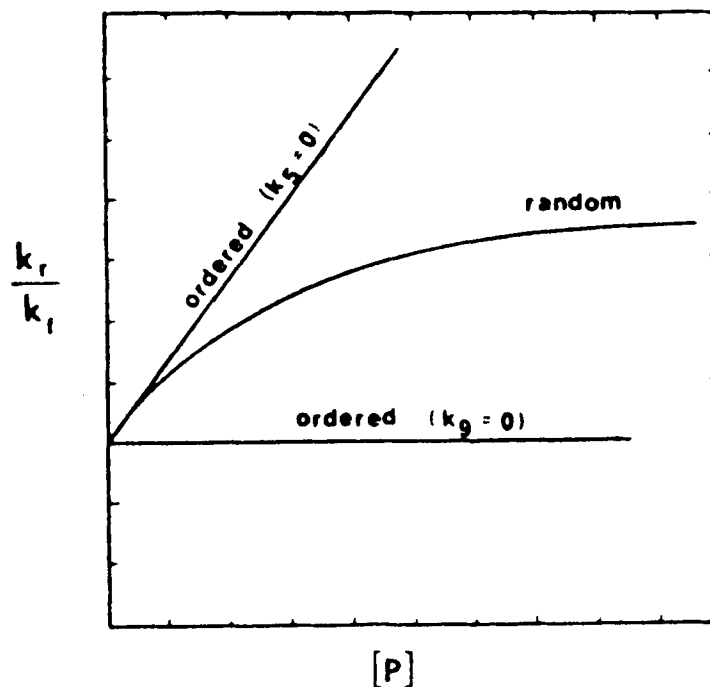


FIGURE 1. Enhancement of the ratio of PIX rate and the net rate of chemical turnover as a function of the concentration of product.

Since the turnover number in the reverse direction ( $V_2/E_t$ ) is equal to  $k_2k_4/(k_2 + k_3 + k_4)$  the lower limit for the ratio of  $k_9$  to  $V_2/E_t$  can be determined as shown in Equation 5.

$$k_9/(V_2/E_t) = k_r/k_t + k_9/k_2 \quad (5)$$

It can also be demonstrated that the value of  $k_{11}$  relative to  $V_2/E_t$  can be determined from the slope and intercept as indicated below:

$$\frac{k_{11}}{(V_2/E_t)} = \left(\frac{1}{K_p}\right) \left(\frac{\text{intercept} + 1}{\text{slope}}\right) \quad (6)$$

where  $K_p$  is the Michaelis constant for the product P.

If arginine were required to be released before fumarate ( $k_9 = 0$ ) then there would be no dependence by  $[P]$  on the ratio of the PIX rate and the net chemical turnover of substrate. This is because fumarate would now be unable to directly influence the partitioning of EPQ. The lower limit for  $k_5$  relative to  $V_2/E_t$  is determined from Equation 7.

$$k_5/(V_2/E_t) = k_r/k_t + k_5/k_2 \quad (7)$$

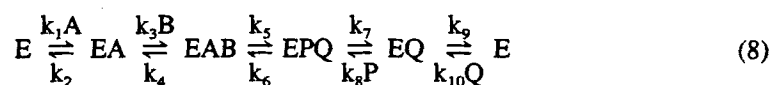
It is readily apparent that the determination of the ratio of the PIX and chemical rate as a function of added product is very useful. The kinetic mechanism is easily determined by inspection of a plot of  $k_r/k_t$  vs.  $[P]$  (see Figure 1). From the limiting values at zero, intermediate, and saturation of product many of the rate constants for the release of both products from the binary and ternary complexes can be obtained. Although the above analysis has been presented for a Uni-Bi kinetic mechanism, similar expressions are easily obtained for more complicated mechanisms using the theory of net rate constants of Cleland.<sup>8</sup>

The analysis of the argininosuccinate lyase reaction was quite informative.<sup>6</sup> At zero fumarate there was no detectable PIX relative to the net formation of products ( $k_r/k_f < 0.15$ ). At higher levels of added fumarate the ratio increased until a plateau was reached with a value of 1.8. It could thus be concluded that the release of products was random since the ratio increased to a limiting value. Since no exchange was observed at low fumarate, the release of at least one of the products (either arginine or fumarate) must be very fast relative to the maximal velocity in the reverse direction. The limiting value of 1.8 at saturating fumarate shows that the release of arginine from the E-arginine-fumarate complex ( $k_5$ ) relative to  $V_r/E_i$  is greater than or equal to 0.5. Therefore, the release of fumarate is very fast ( $k_9/(V_r/E_i) > 6$ ). In summary, these experiments have indicated that argininosuccinatelyase has a random release of products and that fumarate is released at least ten times faster than is arginine from the E-arginine-fumarate complex.

### B. PIX Inhibition

The rate of PIX in enzyme-catalyzed reactions is also dependent on the concentration of the unlabeled substrate. For example, in an ordered Bi-Bi mechanism in which the labeled substrate binds first to free enzyme, saturation with the second substrate will totally suppress the observed PIX rate. This is because saturation with the second substrate totally prevents the labeled substrate from ever dissociating back into solution regardless of whether PIX has occurred within the bound labeled substrate. For example, the PIX reaction catalyzed by *E. coli* carbamyl phosphate synthetase is completely inhibited by high concentration of glutamine and  $\text{NH}_3$ .<sup>2</sup> This observation confirms the ordered kinetic mechanism as deduced from classical initial velocity and product inhibition studies.<sup>9</sup> However, if the addition of the two substrates is random then saturation of the unlabeled substrate will reduce but not totally inhibit the PIX reaction relative to net substrate turnover. If the unlabeled substrate is required to bind prior to the labeled substrate no inhibition of the PIX rate will be observed. Thus, the variation of the PIX rate as a function of the unlabeled substrate can be qualitatively used to determine kinetic mechanisms. These inhibition studies conveniently complement experiments in which the addition of products are used to enhance the PIX rates.

The inhibition of PIX reactions by substrates can also be analyzed quantitatively to obtain microscopic rate constants for the release of substrates from the binary and ternary enzyme complexes. The kinetic expressions have been derived for an ordered Bi-Bi kinetic mechanism as illustrated below.<sup>10</sup>



In this example, A is the substrate with the positionally labeled atoms, and P is the product in which the actual positional exchange occurs. Therefore, the PIX rate relative to the rate for net substrate turnover is determined by the partitioning of the complex EPQ. The substrate B can influence this partitioning by suppressing the conversion of EAB back to EA. The expression for the chemical rate ( $k_f$ ) relative to the PIX rate ( $k_r$ ) as a function of the concentration of [B] is given below:

$$\frac{k_f}{k_r} = \frac{k_7(k_2 k_4 + k_2 k_5 + k_3 k_5 B)}{k_2 k_4 k_6} \quad (9)$$

A plot of  $k_f/k_r$  vs. [B] is therefore a straight line. The slope is equal to  $(k_3 k_5 k_7)/(k_2 k_4 k_6)$  and the intercept is  $k_7(k_4 + k_5)/(k_2 k_4 k_6)$ . It can be easily shown that the microscopic rate constant ( $k_2$ ) for the release of A from the EA complex can be obtained from combination of the slope, intercept, and the Michaelis constant for B as indicated below:

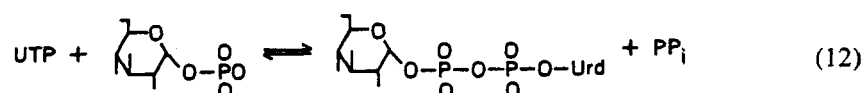
$$\frac{k_2}{(V_1/E_1)} = \left( \frac{1 + \text{intercept}}{\text{slope}} \right) \left( \frac{1}{K_p} \right) \quad (10)$$

The lower limit for the microscopic rate constant for the release of P from the EPQ complex ( $k_7$ ) can be obtained from Equation 11.

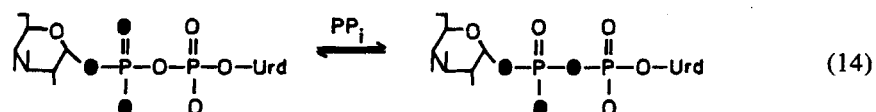
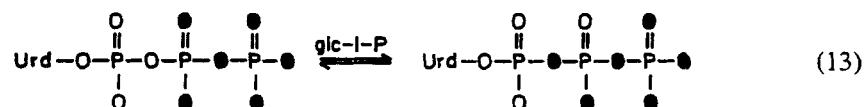
$$\frac{k_7}{(V_2/E_1)} = \frac{k_7}{k_2} + \frac{k_7}{k_4} + \text{intercept} \quad (11)$$

The uncertainty lies in the relative magnitudes of  $k_7$ ,  $k_2$ , and  $k_4$ . Since  $k_2$  relative to  $V_1/E_1$  would be known from Equation 10 this can be partially corrected. If a complementary PIX reaction can be monitored in the reverse direction then  $k_9$  will be determined and an expression analogous to Equation 11 will be obtained that also contains  $k_7$  and  $k_4$  as unknowns. Since two independent equations are obtained with two unknowns the combination will thus result in an exact solution for both  $k_7$  and  $k_4$ . Thus, in principle, all four microscopic rate constants can be determined from PIX experiments in the forward and reverse directions.

Hester et al.<sup>10</sup> have recently reported that independent PIX reactions can be measured in the reaction catalyzed by UDPG pyrophosphorylase. This enzyme catalyzes the following reaction:



Since the reaction proceeds by a nucleophilic attack at the  $\alpha$ -P of UTP by glucose-1-P two independent PIX reactions are measurable as indicated below:



The kinetic mechanism has also been shown to be ordered.<sup>11</sup> UTP binds first followed by glucose-1-P and then  $\text{PP}_i$  is released followed by UDPG. Therefore, glucose-1-P and  $\text{PP}_i$  can be used to suppress the PIX reaction in either direction. In the forward direction glucose-1-P was shown to linearly inhibit the PIX reaction within UTP (see Figure 2). The intercept at low glucose-1-P was  $1.0 \pm 0.20$  and the slope was  $4.0 \text{ mM}^{-1}$ . Utilization of Equations 10 and 11 and the kinetic constants from steady-state measurements have permitted the calculation of  $k_2$  and  $k_7$  to be 40 and  $>1$  times  $V_{\text{max}}$ , respectively. Measurements of the PIX reaction in the reverse direction are in progress.

Clearly, the quantitative analysis of PIX rates as a function of added substrates and products can be very informative. The determination of individual microscopic rate constants would be very difficult to obtain in any other way.

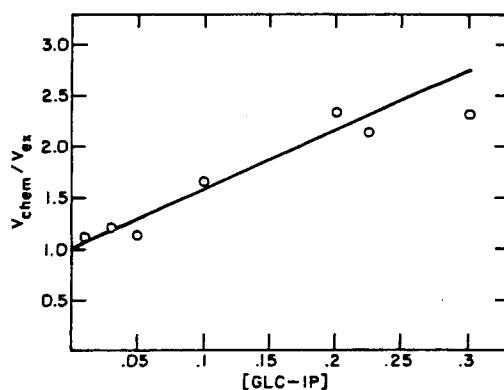
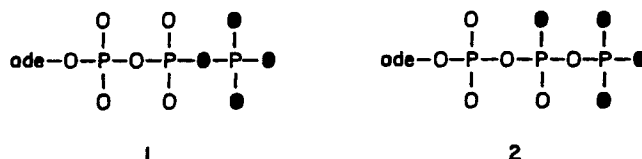


FIGURE 2. Ratio of the rate of net chemical reaction and PIX rate vs. Glc-1P concentration for UDPG pyrophosphorylase.

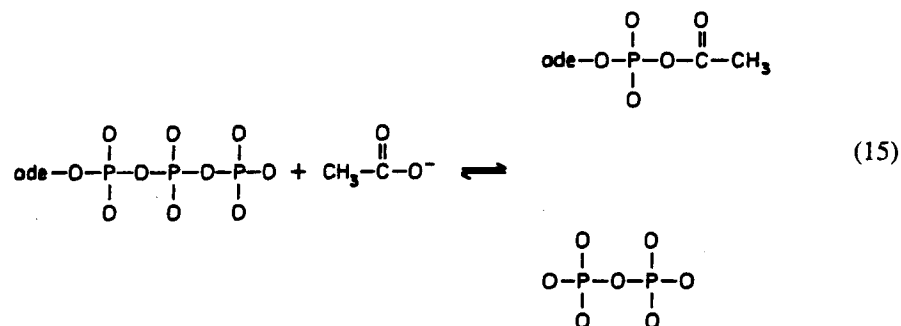
### III. MEASUREMENT OF PIX RATES

To date, the analysis of PIX reactions has been limited to either NMR or mass spectrometry (MS) techniques. The exact procedure has been dictated largely by the amount of material available and the particular exchange reaction being measured. In general, the NMR methods require significantly more material than the mass spectrometry techniques but usually require fewer manipulations. Since the synthesis of labeled substrates suitable for PIX reactions is not particularly difficult or expensive the NMR approach has been favored by most workers in this area.

Midelfort and Rose<sup>3</sup> were the first to utilize MS in the analysis of the PIX reactions of ATP. The first PIX reactions in ATP catalyzed by glutamine synthetase required a method for distinguishing between 1 and 2.

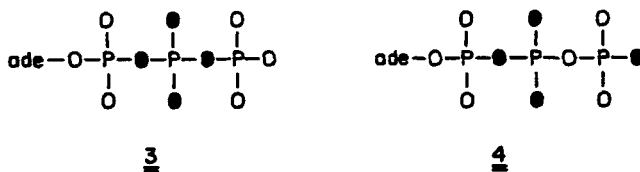


Since no chemical or enzymatic methods were available for removing the  $\gamma$ - $\text{PO}_4$  unit intact, an indirect method had to be devised for determining the extent of  $\beta\gamma$ -bridge to  $\beta$ -nonbridge exchange. The method they devised required both enzymatic and chemical steps. Acetyl-CoA synthetase was added to scramble the  $\beta$  and  $\gamma$  phosphoryl groups of ATP. Acetyl-CoA synthetase catalyzes the adenylation of acetate as shown below:

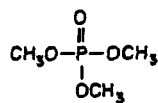




nce the pyrophosphate can leave the enzyme active site and reassociate with the enzyme-bound acetyl-adenylate to reform ATP, the  $\gamma$ - and  $\beta$ -phosphoryl groups will become equilibrated with time. In addition to Structures 1 and 2, compounds 3 and 4 will form.



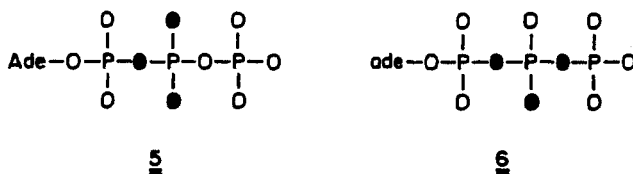
he extent of PIX is presented as the appearance of  $\gamma$ - $\text{PO}_3$  groups (as in 4) with only 1 atom of  $^{18}\text{O}$ . The equilibrated ATP sample is then reacted with dihydroxyacetone and glycerokinase to cleave the  $\gamma$ - $\text{PO}_3$  group. The resultant dihydroxyacetone phosphate is cleaved by hydroxide ion to form  $\text{HPO}_4^{2-}$ . The phosphate is permethylated with  $\text{CH}_3\text{I}$  to form trimethylphosphate.



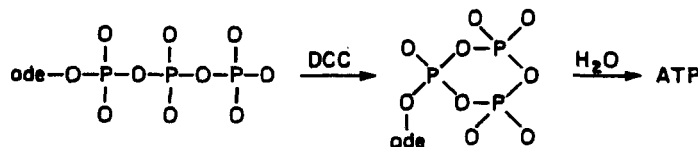
$m/e = 141$

he mass ratios of the trimethylphosphate are analyzed by conventional MS. The appearance of a signal at  $m/z$  143 (1 atom of  $^{18}\text{O}$ ) signifies the occurrence of the exchange from a  $\beta$ -bridge to a  $\beta$ -nonbridge position. If 1 and 2 have become fully equilibrated then the ratio of the  $m/z$  143 and  $m/z$  147 peaks will be 0.67. Suitable corrections have to be made to correct for the precise amount of the original labeling of  $^{18}\text{O}$ .

More recently, Webb<sup>12</sup> devised an alternate method for measuring the rate of  $\beta$ - $\gamma$ -bridge to  $\beta$ -nonbridge exchange in nucleotide triphosphates. This method was developed because the method of Midelfort and Rose<sup>3</sup> was restricted to exchange reactions of ATP but was not applicable to other nucleotide triphosphates. The method of Webb<sup>12</sup> utilizes ATP labeled as 5 and follows the label from the  $\beta$ -nonbridge to  $\beta$ - $\gamma$ -bridge position (see 6).

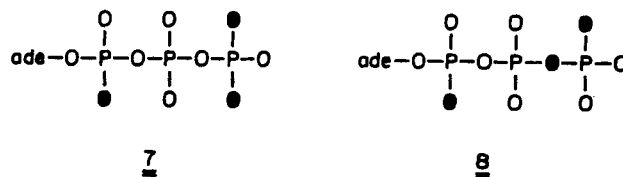


he  $\beta$ - and  $\gamma$ -phosphoryl groups are first equilibrated by the action of dicyclohexylcarbodiimide (DCC) and pyridine via the cyclophosphate intermediate as illustrated below:



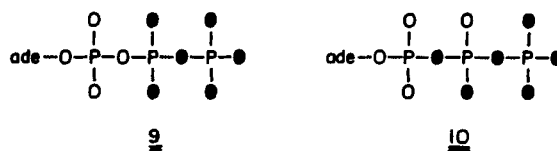
he attack by water is essentially random at either the  $\beta$  or  $\gamma$  phosphorus atom to produce the  $\beta$ - and  $\gamma$  scrambled ATP (5 and 7). The addition of DCC and pyridine to a mixture of 5 and 6 would produce 6 and 8 in addition to 5 and 7.





The terminal  $\gamma\text{-PO}_3$  is cleaved in the presence of glycerokinase and *d*-glyceraldehyde to produce  $\text{HPO}_4^{2-}$ , which is then permethylated as before to form trimethylphosphate. The extent of the original  $\beta\gamma$ -bridge to  $\beta$ -nonbridge exchange is determined by the ratio of the peaks at  $m/z$  143 and  $m/z$  145. At equilibrium this ratio would be 1:2.

The recent availability of fast atom bombardment mass spectrometry (FAB-MS) has made the analysis of phosphorylated nucleotides even more routine. FAB-MS is able to determine the molecular ion mass ratios of phosphates and nucleotides without prior derivitization. Hilscher et al.<sup>13</sup> used FAB-MS to monitor the PIX reactions catalyzed by argininosuccinate synthetase and acetyl-CoA synthetase. Both of these enzymes catalyze an attack at the  $\alpha\text{-P}$  of ATP to form an adenylated intermediate and pyrophosphate. The expected PIX reactions were initiated with labeled ATP in the  $\beta$ -nonbridge position (9) and the appearance of an  $\alpha\beta$ -bridge labeled ATP (10) was monitored.



Although FAB-MS can determine the  $^{18}\text{O}$  content of ATP samples with as little as 10 nmol of material, ATP does not fragment in such a way that 9 and 10 can be easily distinguished. To circumvent this problem, Hilscher et al.<sup>13</sup> quenched their incubation reactions with a mixture of glucose, hexokinase, and adenylate kinase. These reagents successively removed the  $\gamma$ - and  $\beta$ -phosphoryl groups, leaving the AMP with the  $\alpha\beta$ -bridge oxygen. Therefore, the original ATP molecules which have undergone positional exchange will contain one  $^{18}\text{O}$  in the resultant AMP, while those that have not will contain none. The resolving power of FAB-MS is illustrated in Figure 3, where the negative ion mass spectrum of AMP is presented containing the three stable isotopes of oxygen. This spectrum required approximately 10 nmol of total material. To date, this approach has only been utilized with a reaction center at the  $\alpha\text{-P}$  of ATP. Other nucleotides can also be utilized if apyrase is used to cleave the  $\beta$ - and  $\gamma$ -phosphoryl groups of the nucleotide triphosphates. FAB-MS could also be used in enzymatic reactions at the  $\gamma\text{-P}$  of ATP if the nucleotides were processed as described by Midelfort and Rose<sup>3</sup> or Webb.<sup>12</sup> The resultant phosphate could then be analyzed directly without conversion to the trimethyl phosphate derivative.

#### A. NMR

The application of NMR to the analysis of PIX reactions within ATP was initiated by Cohn and Hu<sup>14</sup> when they discovered that the substitution of an  $^{18}\text{O}$  for an  $^{16}\text{O}$  in phosphate and phosphate esters induced a  $\sim 0.02$  ppm upfield chemical shift in the  $^{31}\text{P}$  NMR resonance per oxygen substituted. This effect is dramatically illustrated in Figure 4, where the  $^{31}\text{P}$  NMR spectrum of a sample of inorganic phosphate labelled with  $\sim 78\%$   $^{18}\text{O}$ . The five possible species containing 0 to 4 atoms of  $^{18}\text{O}$  are clearly separated. This discovery enabled the PIX reactions at the  $\alpha$ - and  $\gamma$ -phosphoryl groups to be easily determined by inspection of the  $^{31}\text{P}$  NMR spectrum of the region of interest. For example, the exchange of label from

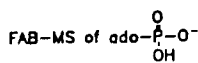


FIGURE 3. FAB-ms of AMP labeled with  $^{18}\text{O}$  and  $^{17}\text{O}$ .

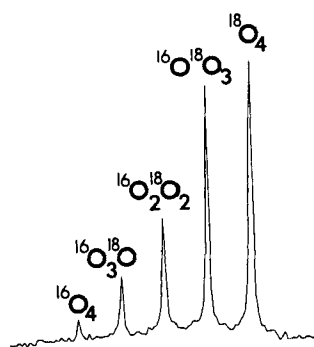


FIGURE 4.  $^{31}\text{P}$ -NMR spectrum at 145 MHz of inorganic phosphate randomly labeled with 78%  $^{18}\text{O}$  and 22%  $^{16}\text{O}$ .

the  $\beta\gamma$ -bridge position to a  $\beta$ -nonbridge position (as in **1** to **2**) would result in the decrease of the signal for the  $\gamma$ -P with 4  $^{18}\text{O}$  atoms and an increase in the signal for the  $\gamma$ -P with 3  $^{18}\text{O}$  atoms.

This NMR approach has been applied to many enzymatic PIX reactions. The limitations of this technique are such that approximately 5 to 10  $\mu\text{mol}$  of labeled ATP are required per analysis. This is significantly more material than the comparable MS methods. The advantage of the NMR methodology is that essentially no exotic sample preparation is required. In order to get the maximum possible resolution the sample must be titrated to approximately pH 9 and all of the divalent cations must be sequestered. This must be done in order to minimize the exchange broadening by metals and protons. This exchange broadening has in general prevented the use of NMR to continuously monitor the PIX reactions. However, Raushel and Villafranca<sup>2</sup> were able to continuously monitor the time course of a PIX reaction within carbamyl phosphate catalyzed by carbamyl phosphate synthetase (see Scheme III).

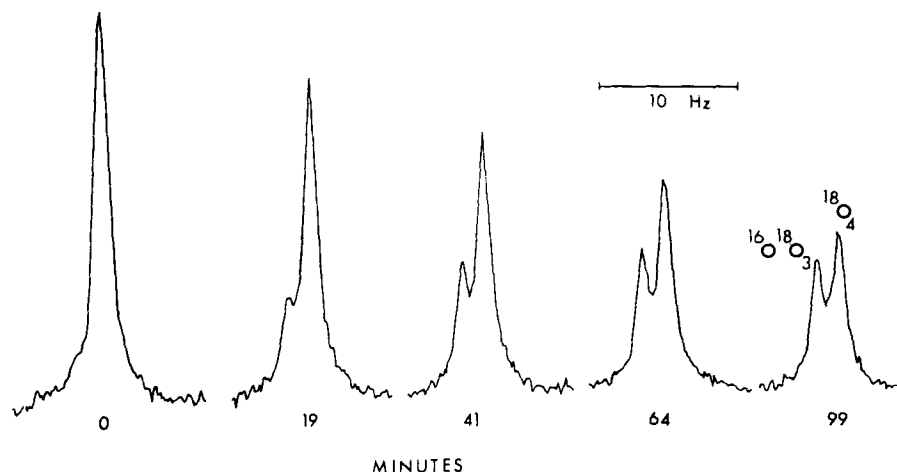
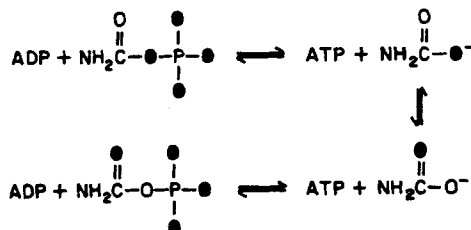


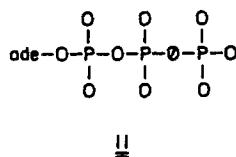
FIGURE 5.  $^{31}\text{P}$ -NMR spectra at 81 MHz of carbamyl-P labeled with  $^{18}\text{O}$  after incubation with carbamyl-P synthetase and ADP for the indicated times.



Scheme III

Shown in Figure 5 is the  $^{31}\text{P}$  NMR spectrum of carbamyl phosphate at various times after incubation with ADP and carbamyl phosphate synthetase. This PIX reaction demonstrates the transient formation of ATP and carbamate. The carboxyl group of carbamate is able to rotate and thus torsionally scramble the  $^{18}\text{O}$  and  $^{16}\text{O}$  atoms. In this particular case the enzyme catalyzed PIX is four times faster than the net chemical formation of ATP.

More recently, Reynolds et al.<sup>15</sup> have developed a new NMR method for the analysis of PIX reactions within ATP. The Kenyon group has synthesized ATP with the  $\beta\gamma$ -bridge oxygen labeled with  $^{17}\text{O}$  (species 11). Upon PIX equilibration, transfer



will occur to the  $\beta$ -nonbridge position. Earlier, Tsai<sup>16</sup> showed that the introduction of an  $^{17}\text{O}$  nucleus adjacent to a phosphorus atom broadened the  $^{31}\text{P}$  NMR signal for the phosphorus into the baseline. This is due to the quadrupolar coupling of the spin 5/2  $^{17}\text{O}$  nucleus with the phosphorus. Therefore, as the exchange reaction proceeds, the high-resolution signal for the  $\gamma$ -P increased in intensity. The potential advantage of this new methodology is that a low-field NMR spectrometer is sufficient. The  $^{18}\text{O}$ -method of Cohn and Hu<sup>14</sup> generally requires field strengths in excess of 4.7 T (200 MHz for  $^1\text{H}$ ) in order that sufficient resolution

between signals is obtained. With the Kenyon method this is not a requirement since the shift of an  $^{17}\text{O}$  nucleus away from the phosphorus atom results in the appearance of the signal and thus high resolution is not required. The shortfalls of this method are the difficult synthesis of the  $\beta\gamma$ -bridge ATP, and the fact that  $^{17}\text{O}$  is only available at 60% incorporation. Thus, starting ATP is only available at 60% incorporation and will contain a mixture of  $^{16}\text{O}$ ,  $^{17}\text{O}$ , and  $^{18}\text{O}$ .

#### IV. APPLICATION OF PIX EXPERIMENTS TO SPECIFIC ENZYME REACTIONS

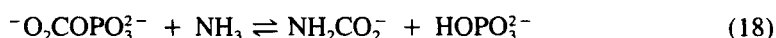
##### A. Enzymes that Catalyze a PIX Reaction

###### 1. Carbamyl-Phosphate Synthetase

Carbamyl-phosphate synthetase from *E. coli* catalyzes the following reaction:



Anderson and Meister<sup>17</sup> originally proposed that the mechanism for carbamyl-phosphate formation consisted of at least three separate steps as shown below:



There are thus two intermediates in this mechanism: carboxyphosphate and carbamate. PIX experiments have been completed on this enzyme by three different research groups in attempts to provide definitive evidence for these two intermediates.<sup>2,2a,15</sup>

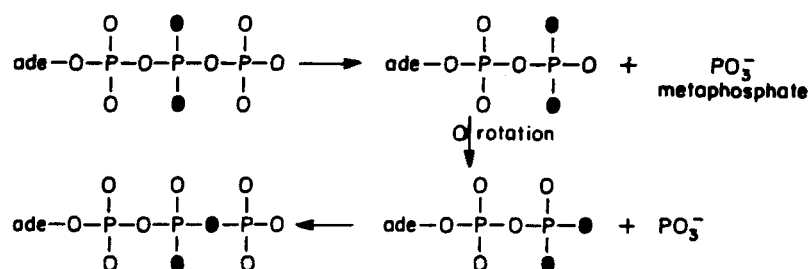
In the absence of an ammonia source the enzyme will catalyze the bicarbonate-dependent hydrolysis of ATP to ADP and  $\text{P}_i$ . This hydrolytic activity is presumed to be due to the instability of the carboxyphosphate formed in the first step of the mechanism. PIX experiments were used to probe for the formation of carboxyphosphate and to determine the partitioning parameters of the E-ADP-carboxyphosphate complex. The ratio of the exchange rate of an oxygen label from the  $\beta\gamma$ -bridge position to the  $\beta$ -nonbridge position of ATP relative to net rate of ATP hydrolysis varied from 0.46 to 1.7.<sup>2,2a,15</sup> Therefore, the E-ADP-carboxyphosphate complex releases a product into solution about as fast as ATP is resynthesized and released into the bulk solution.

The second intermediate, carbamate, was probed by following the PIX of an  $^{18}\text{O}$  label within carbamyl-phosphate (see Scheme III).<sup>2a</sup> In the presence of carbamyl-phosphate and ADP the enzyme will catalyze the reverse of the third step to form ATP. Phosphate is apparently unable to react with carbamate and thus the final products are  $\text{NH}_3$  and  $\text{HCO}_3^-$ . This was the first reported PIX experiment that took advantage of the symmetry in a carboxyl group. The PIX rate was found to be 4.0 times faster than the net rate of formation of ATP. Therefore, it could be concluded that the enzyme-bound carbamate was reacting with ATP to reform and release carbamyl-phosphate much faster than ATP was released into the bulk solution.

###### 2. Pyruvate Kinase

Pyruvate kinase catalyzes the transfer of the phosphoryl group from PEP to ADP to synthesize ATP and pyruvate. The transfer occurs without the occurrence of a phosphoen-

zyme intermediate. Lowe et al.<sup>18</sup> used this enzyme to probe whether the transfer of the phosphoryl group occurred via a metaphosphate intermediate (i.e., dissociative mechanism). If metaphosphate could form from ATP in the active site in the absence of pyruvate then a PIX reaction should occur from a  $\beta$ -nonbridge position to the  $\beta\gamma$ -bridge position as shown below:

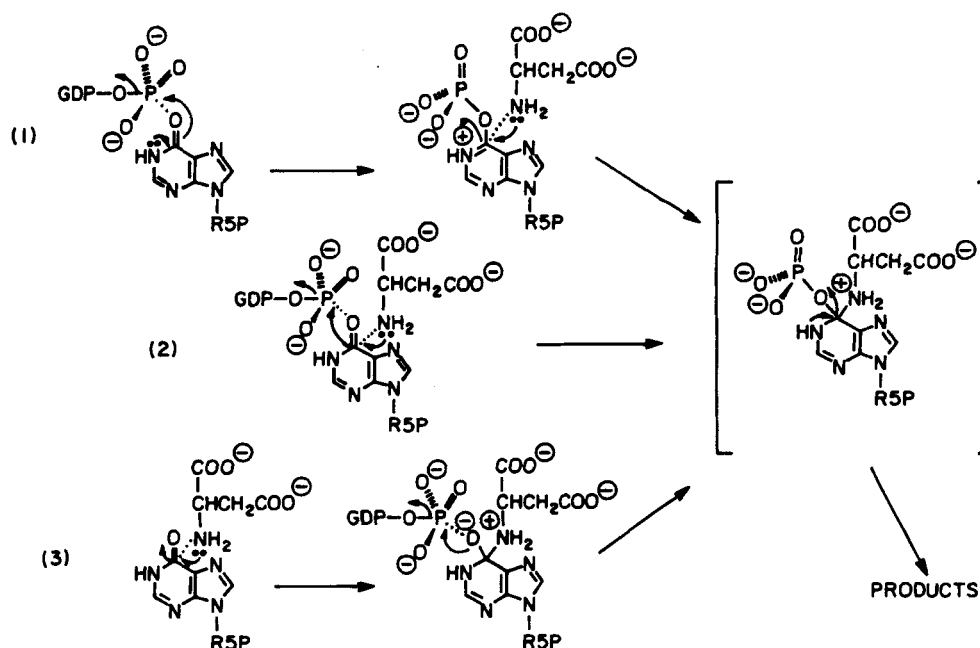


With commercially obtained pyruvate kinase, Lowe et al.<sup>18</sup> were able to demonstrate that a PIX reaction occurred. The rate of exchange when pyruvate was present was 18-fold faster than when pyruvate was omitted. All exchange was lost when PEP was added to the reaction mixture to prevent ATP from binding to pyruvate kinase. Since pyruvate kinase catalyzed a PIX reaction in the absence of the second substrate, pyruvate, it was concluded that a metaphosphate intermediate was formed and the mechanism was dissociative rather than associative.

These experiments have since been repeated by Hassett et al.<sup>19</sup> with a more highly purified preparation of pyruvate kinase from rabbit muscle. They concluded that a contaminant in the commercial enzyme was responsible for the PIX reaction and that there is no reason to suggest that pyruvate kinase catalyzed the formation of metaphosphate via a dissociative mechanism. This result is also now in accord with the lack of PIX within ATP in the absence of some acceptor molecule by creatine kinase<sup>20</sup> and hexokinase.<sup>21</sup>

### 3. Adenylosuccinate Synthetase

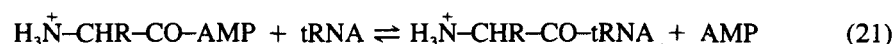
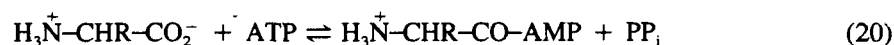
Adenylosuccinate synthetase catalyzes the formation of adenylosuccinate from GTP, IMP, and aspartate. Three mechanisms have been proposed for this reaction as indicated below:



In mechanism 1 GTP phosphorylates the carbonyl oxygen of the IMP. The  $\alpha$ -amino group of aspartate then displaces the activated phosphate to form the final product adenylosuccinate. In mechanism 2 the reaction is concerted. Phosphorylation of the inosine base occurs simultaneously with attack by aspartate. In mechanism 3 the  $\alpha$ -amino group of aspartate attacks the C-6 of IMP creating an oxyanion intermediate. This intermediate is then phosphorylated by GTP and finally loses  $P_i$  to form the product adenylosuccinate. Only mechanism 1 would result in the positional exchange of an  $^{18}O$  at the  $\beta\gamma$ -bridge position to the  $\beta$ -nonbridge position in the absence of aspartate. Bass et al.<sup>22</sup> synthesized  $[\gamma\text{-}^{18}O_4]\text{GTP}$  to test as a PIX probe of the adenylosuccinate synthetase reaction. They found no exchange with GTP alone but substantial exchange upon addition of enzyme, GTP, and IMP. These results rule out both mechanism 2 and 3 since both of these mechanism require the presence of aspartate before any PIX can occur.

#### 4. Aminoacyl-tRNA Synthetases

The aminoacyl-tRNA synthetases are a group of enzymes that catalyze the condensation of amino acids to their respective tRNA. The mechanism for all of these enzymes appears to involve the activation of the amino acid by adenylation with ATP to form an aminoacyl-adenylate and pyrophosphate. The aminoacyl-adenylate then reacts directly with the cognate tRNA. These reactions are summarized below:

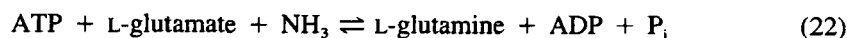


The formation of the aminoacyl-adenylate has been demonstrated by direct isolation<sup>23</sup> and by an exchange reaction between ATP and  $\text{PP}_i$ <sup>24</sup> in the absence of any added tRNA. PIX reactions have been completed on the valyl-, methionyl-, isoleucyl-, and tyrosyl-enzymes by Cohn<sup>25</sup> and Lowe.<sup>26-28</sup> Smith and Cohn<sup>25</sup> were able to demonstrate that valyl-tRNA synthetase is able to catalyze a "direct interchange reaction" in the presence of ATP and an amino acid. This reaction results from the direct interchange of the  $\beta$ - and  $\gamma$ -phosphoryl group of ATP. Presumably this reaction occurs via the complete "flipping" of bound pyrophosphate within the active site after the formation of the aminoacyl-adenylate. They have further demonstrated that this reaction is not dependent on the prior dissociation-reassociation of the pyrophosphate to the active site. Thus far, this is one of few examples of a symmetrical molecule that is able to completely reorientate itself within the active site of an enzyme.

In a series of three nearly identical papers, Lowe et al.<sup>26-28</sup> have examined the PIX reactions catalyzed by methionyl-, tyrosyl-, and isoleucyl-tRNA synthetases. With all three enzymes it was established that no PIX occurred within ATP in the absence of an amino acid nor did it occur when an analogue of the amino acid was added to the reaction mixture (isoleucinol, tyrosinol, and methioninol). These experiments demonstrated that the enzyme is not adenylated upon addition of ATP. This observation is also supported by the net inversion of configuration of the  $\alpha$ -P during the course of the reaction.<sup>26-28</sup> However, when the amino acid was added in addition to the ATP all three enzymes efficiently catalyzed the positional isotope exchange from the  $\beta$ -nonbridge to the  $\alpha\beta$ -bridge position. These results clearly demonstrate the formation of the aminoacyl-adenylate and pyrophosphate in the absence of added tRNA.

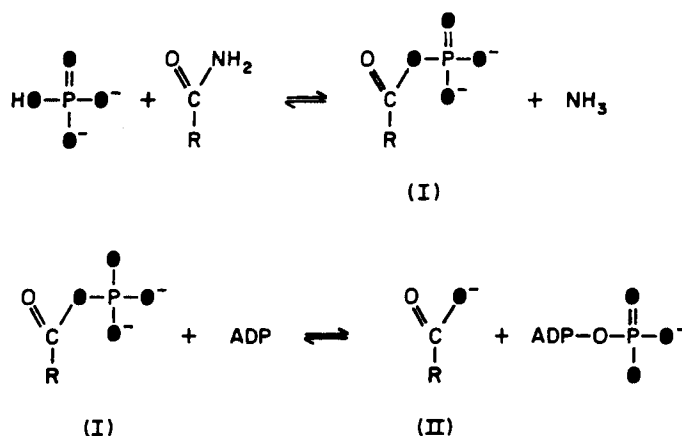
#### 5. Glutamine Synthetase

The reaction catalyzed by glutamine synthetase is



The question of whether  $\gamma$ -glutamyl phosphate was an intermediate in this reaction has been a point of discussion for many years. Midelfort and Rose<sup>3</sup> developed the PIX experiments, that are the subject of this article, to provide the first definitive evidence for the viability of  $\gamma$ -glutamyl phosphate in this enzyme-catalyzed reaction. Later studies of Meek et al.<sup>29</sup> established that  $\gamma$ -glutamyl phosphate is a kinetically competent intermediate. Stokes and Boyer<sup>30</sup> demonstrated that oxygen can be transferred from  $P_i$  to glutamine, further demonstrating the existence of a  $\gamma$ -glutamyl phosphate intermediate.

In an examination of the "timing" of the formation of this intermediate, i.e., before or after the third substrate  $NH_3$  binds, Clark and Villafranca<sup>30a</sup> employed isotope-exchange enhancement studies. In this work the reverse biosynthetic reaction of glutamine synthetase was studied.



The ratio  $v_{ex}/v_{rxn}$  was modulated by adding varying amounts of  $NH_4^+$ . The isotope traced was  $^{18}O$ , introduced into the reaction in the form of  $KH_2P^{18}O_4$ . As the reaction proceeded,  $^{18}O$  was depleted due to the reactions depicted in the scheme above.

The formation of  $\gamma$ -glutamyl phosphate from ATP and L-glutamate may occur in one of three ways. It may form only when  $NH_4^+$  is bound to the enzyme surface or only when  $NH_4^+$  is absent from the enzyme, or there may be no requirement for the presence or absence of  $NH_4^+$  at all. In addition, these three cases may be further subdivided to account for random or ordered binding of ATP and L-glutamate. Kinetic studies have indicated that the glutamine synthetase reaction is ordered,<sup>31</sup> while isotope-exchange experiments have detected apparent random behavior in the binding of ATP and L-glutamate.<sup>32</sup>

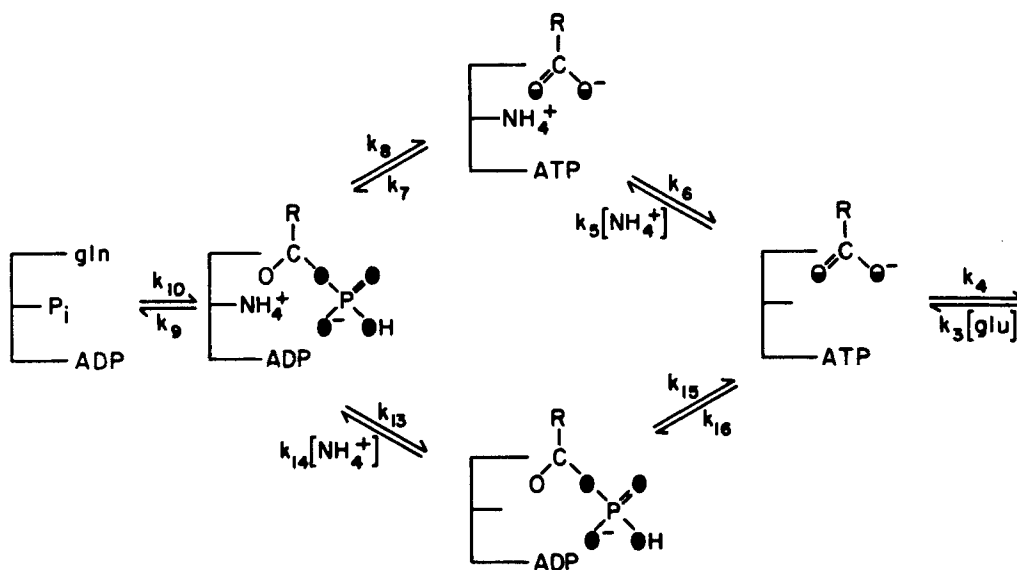
First, let us consider the case in which  $\gamma$ -glutamyl phosphate can be formed only by the enzyme form containing bound  $NH_4^+$ . If the mechanism is strictly ordered, then in the simplest experiment, ADP and L-gln can be held at saturating levels while  $P_i$  is subsaturating. The  $NH_4^+$  concentration will be varied, while the concentration of ATP and L-glu is maintained at 0 by the presence of hexokinase and glutamic dehydrogenase.

Under these conditions, a plot of  $v_{ex}/v_{rxn}$  vs. ammonium ion concentration would be a straight line with positive intercept and slope as in curve I of Figure 6A. The intercept on this plot is the partition ratio between the fraction of  $E \cdot ATP \cdot Glu \cdot NH_4^+$  that reverses to form  $\gamma$ -glutamyl phosphate and the fraction from which  $NH_4^+$  dissociates. In addition, the slope of the plot divided by the intercept is the partition between the fraction of  $E \cdot ATP \cdot Glu$  that combines with ammonium ion and the fraction from which L-glu dissociates.

If  $\gamma$ -glutamyl phosphate can be formed only in the absence of enzyme-bound  $NH_4^+$ , the relation between  $v_{ex}/v_{rxn}$  and ammonium ion concentration is nonlinear. As the concentration of  $NH_4^+$  increases to saturating levels (effective infinity), the ratio  $v_{ex}/v_{rxn}$  increases to a limiting value. A plot expected for this type of mechanism is shown in curve II of Figure



6A. The asymptote represents the partitioning of E·ATP·Glu between the fraction that reacts to form  $\gamma$ -glutamyl phosphate and the fraction from which L-glu dissociates.



Scheme IV

Scheme IV shows a section of the reaction pathway when there is no absolute requirement for the presence or absence of  $\text{NH}_4^+$  during the formation of  $\gamma$ -glutamyl phosphate. In this scheme, either the E-ADP- $\text{NH}_4^+$ - $\gamma$ -glutamyl phosphate complex may undergo a chemical transformation to the E·ATP·Glu· $\text{NH}_4^+$  complex, as depicted in the top branch, or ammonium ion may dissociate, as in the bottom branch. Isotopic exchange occurs in two places in this mechanism: when the E·ATP·Glu· $\text{NH}_4^+$  complex reverses to form E-ADP- $\text{NH}_4^+$ - $\gamma$ -glutamyl phosphate and when the E·ATP·Glu complex reacts to form E-ADP- $\gamma$ -glutamyl phosphate. Because the chemical transformations occur in a loop in which all steps are reversible, it is not possible to use net rate constants to derive a simple expression for  $v_{\text{ex}}/v_{\text{rxn}}$ . The behavior for this mechanism may be a mixture of the characteristics of the other two, depending on the actual values of the rate constants and the concentration of the modifier.

Figure 6B shows the data from these experiments. As the concentration of ammonium ion is increased, both the velocity of exchange and the velocity of net reaction decrease. However, the rate of exchange decreases faster initially than the velocity of net reaction, reaching a minimum in the range of 1 to 2 mM ammonium ion. This behavior was also observed in other experiments covering lower ammonium ion concentrations. At higher concentrations of  $\text{NH}_4^+$ , the velocity of reaction decreases faster than the velocity of exchange, so the ratio  $v_{\text{ex}}/v_{\text{rxn}}$  begins to rise. The increase in  $v_{\text{ex}}/v_{\text{rxn}}$  is a linear function of the concentration of  $\text{NH}_4^+$ .

The data depicted in Figure 6B clearly do not correspond with the predictions for either of the simple mechanisms considered previously. Some characteristics of the "mixed" mechanism depicted in Scheme IV can be predicted at extremes of  $\text{NH}_4^+$  concentration. In the strict absence of ammonium ion, all of the exchange observed must result from the reversal of E·ATP·Glu· $\text{NH}_4^+$  to E-ADP- $\text{NH}_4^+$ - $\gamma$ -glutamyl phosphate. As the concentration of ammonium ion is increased, the bottom branch in the pathway will contribute to the exchange and net reactions. As ammonium ion concentration continues to increase, the bottom pathway eventually will be "shut off" as the ammonia-release steps (the steps associated with rate

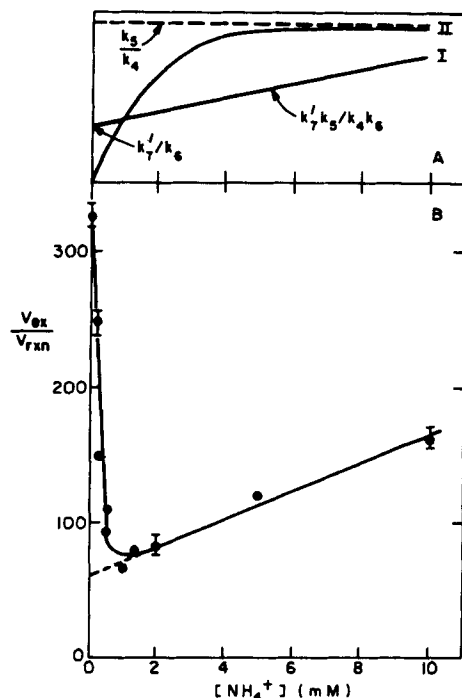


FIGURE 6. (A) Theoretical plot of  $v_{ex}/v_{rxn}$  vs.  $[NH_4^+]$  for various mechanisms of the glutamine synthetase reaction. See text for details. (B)  $v_{ex}/v_{rxn}$  vs.  $[NH_4^+]$  data for glutamine synthetase. See text for details.

constants  $k_6$  and  $k_{13}$ ) become insignificant relative to the ammonia-binding steps. When such conditions apply, the system will behave similarly to a nonbranched mechanism and the ratio  $v_{ex}/v_{rxn}$  will increase as a linear function of the concentration of  $NH_4^+$ .

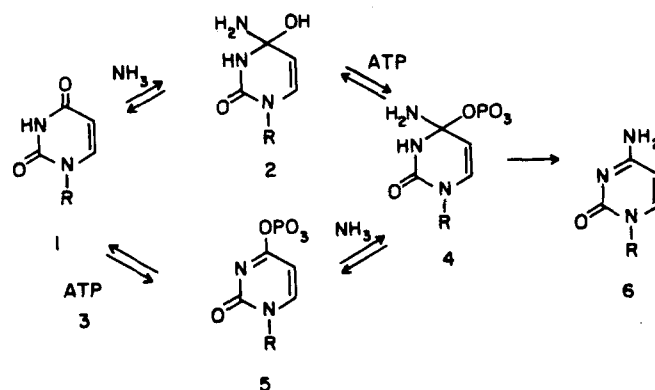
The data in Figure 6B can be interpreted in terms of these predictions. At low ammonia concentrations,  $v_{ex}/v_{rxn}$  is very sensitive to small changes in the  $NH_4^+$  concentration. When the concentration increases slightly, increased net reaction occurs through flux through the bottom part of the reaction scheme. It should be mentioned that this region of extreme sensitivity to concentration brackets the  $K_m$  value, providing the enzyme with very precise control of reaction rates. As the concentration of  $NH_4^+$  continues to increase, a point is reached when flux through the bottom of the pathway decreases since formation of the E-ADP- $\gamma$ -glutamyl phosphate complex is inhibited. After the bottom branch is essentially shut off, the mechanism mimics the strictly ordered mechanism in which ammonia binding and dissociation occur only with the enzyme complex containing ATP and L-glutamate. The ratio  $v_{ex}/v_{rxn}$  rises as a linear function of ammonia concentration under these conditions, as is depicted in our data.

If it is assumed that this linear portion of the graph represents the behavior of the top pathway in the mechanism, it is possible to fit a straight line through that portion of the data. If that line is extrapolated back to zero ammonium ion, as shown by the dashed line in Figure 6B, we can compute the same quantities as for the simpler, nonbranched mechanism. For the experiment depicted in Figure 6B the intercept representing the partition of the E-ATP-Glu- $NH_4^+$  complex between the fraction that undergoes reaction and the fraction from which ammonia dissociates is approximately 60. The slope of the line divided by the intercept, representing the partition of the E-ATP-Glu complex, is 0.17.

It also has been reported that the ratio of the turnover number for the forward biosynthetic reaction ( $V_f/E_i$ ) to the turnover number for the reverse biosynthetic reaction ( $V_r/E_i$ ) of glutamine synthetase is approximately 8 and that the rate-limiting step for the forward biosynthetic reaction is the release of the product MgADP from the E·MgADP complex.<sup>29</sup> Our results are consistent with those observations in that the partition of the E·ATP·Glu·NH<sub>4</sub><sup>+</sup> complex proceeds at least 50 to 60 times faster in the forward direction than in the reverse. Thus, the amount of E·ATP·Glu·NH<sub>4</sub><sup>+</sup> complex that undergoes conversion to E·ADP·NH<sub>4</sub><sup>+</sup>·γ-glutamyl phosphate is more than 50 times that from which the substrate dissociates. Because the ratio of the forward to reverse reactions for this subsection of the mechanism is so much larger than the ratio of net forward reaction to net reverse reaction, the conversion of ATP and L-glutamate to ADP and γ-glutamyl phosphate cannot be the rate-limiting step in the reaction.

#### 6. CTP Synthetase

CTP synthetase from *E. coli* catalyzes the amidotransferase reaction given in Scheme V. The reaction was thought to proceed<sup>33</sup> by the attack of ammonia (alone or generated from glutamine) on the 4-carbon atom of UTP (1) to yield the carbinolamine 2, followed by phosphoryl transfer from ATP (3) to the hydroxyl group of 2. Release of phosphate from compound 4 completes the reaction (Scheme V, upper pathway). The role of ATP is, therefore, to facilitate the removal of water from the carbinolamine, 2.



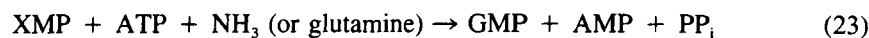
The evidence used to support this idea was the reported lack of ATP-ADP exchange ( $\leq 1\%$  of  $V_{max}$ ) both in the presence and absence of UTP.<sup>33</sup> In addition, transfer of <sup>18</sup>O from 4'-[<sup>18</sup>O] UTP to P<sub>i</sub> was catalyzed by the enzyme,<sup>33</sup> suggesting the formation of a phosphorylated UTP intermediate as part of the mechanism. Thus, these two experiments taken together were interpreted in terms of the mechanism shown in the top branch of Scheme V in which NH<sub>3</sub> must be present for phosphorylation to occur. However, these criteria alone have been shown to be insufficient to decide among various enzymic mechanisms that may involve tightly bound intermediates.

To address this mechanistic problem, von der Saal et al.<sup>34</sup> showed that CTP synthetase from *E. coli* catalyzes exchange of <sup>18</sup>O from the βγ-bridge position of [γ-<sup>18</sup>O<sub>4</sub>] ATP into the β-nonbridge position. This positional isotope exchange occurs in the presence of UTP and MgCl<sub>2</sub> but in the absence of NH<sub>3</sub>. The enzyme also has an ATPase activity in the presence of UTP that occurs under conditions that are identical to those used in the PIX experiments. These data provide evidence for the stepwise nature of the reactions catalyzed by CTP synthetase with the initial step involving phosphorylation of UTP by ATP (bottom branch of Scheme V). The relative rate of the isotope-exchange reaction is ~3 times faster

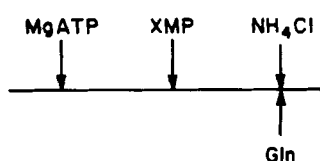
than the ATPase reaction, but the isotope-exchange rate is ~3% of the overall rate in the presence of  $\text{NH}_3$ . These results are consistent with the ATPase reaction involving attack of water on the phosphorylated intermediate (4-phospho-UTP). The PIX reaction is independent of the UTP concentration above saturating levels, demonstrating that the order of addition of substrates is UTP followed by ATP and then  $\text{NH}_3$ .

### 7. GMP Synthetase

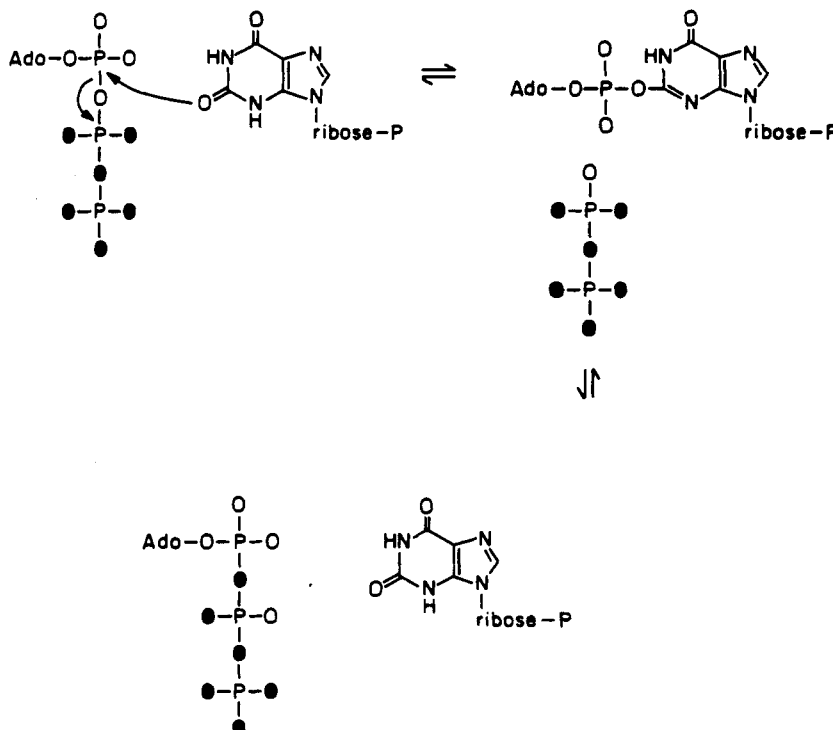
The reaction catalyzed by GMP synthetase is



von der Saal et al.<sup>35</sup> investigated the kinetic mechanism of *E. coli* GMP synthetase by determining the initial velocity patterns of MgATP, XMP, and  $\text{NH}_3$  (or glutamine as nitrogen source). The data are consistent with the ordered addition of MgATP followed by XMP and then  $\text{NH}_3$  (or glutamine).



This mechanism was also confirmed by studying the PIX in the substrate ATP. The PIX reaction given below occurs in the presence of XMP and  $\text{Mg}^{2+}$ . The exchange reaction did not require  $\text{NH}_3$ .



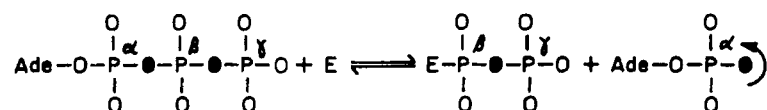
In this study, the order of addition of substrates MgATP and XMP was tested by following the substrate concentration dependence of the PIX reaction. Thus, XMP, the substrate that does not undergo PIX, was varied. The PIX rate increased as XMP increased, then decreased as XMP reached saturating levels. These are the predicted results if MgATP binds first and XMP second in an ordered reaction mechanism. The enzyme also catalyzes an ATP/PP<sub>i</sub> exchange reaction in the absence of NH<sub>3</sub>. All these data taken together support a mechanism in which an adenyl-XMP intermediate is formed in the first step of the reaction.

#### 8. Pyruvate-Phosphate Dikinase

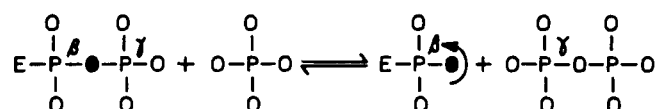
Based on several kinetic and isotope-exchange experiments, this reaction is thought to proceed in a stepwise manner with the intermediate formation of pyrophosphoryl and phosphoryl enzyme species. The equations below describe these three reactions.



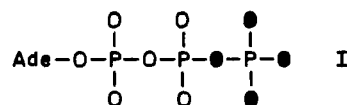
Several PIX experiments have been done<sup>36</sup> to test for formation of E-PP in Reaction 24. For this study, oxygen isotopes in the α-P nonbridge positions have to be different from the isotope in the αβ-bridge position:



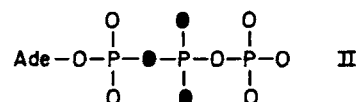
For partial Reaction 25, the same is true for the β-nonbridge and the βγ-bridge positions.



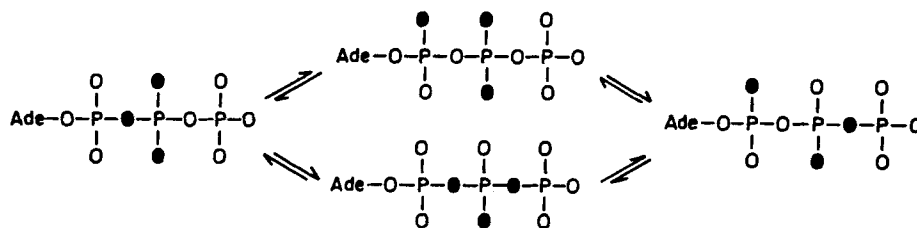
The <sup>18</sup>O-labeled ATP for the latter reaction is compound I



while compound II was used to study both partial reactions.



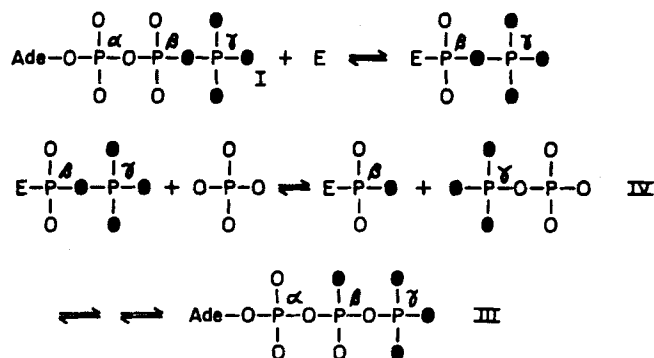
In these experiments, PIX between the αβ-bridge and α-nonbridge oxygen atoms of ATP II was detected when no phosphate was added (upper part of Scheme VI).



Scheme VI

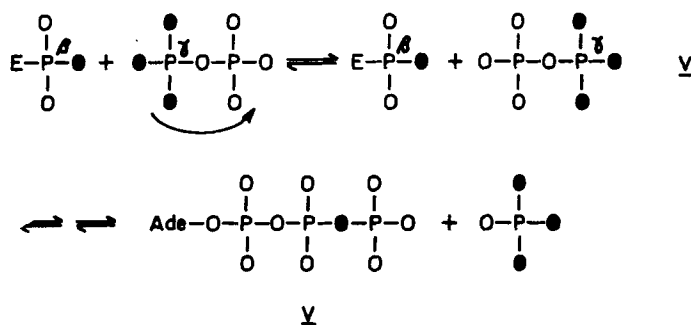
At the same time, however, PIX occurs between the  $\beta\gamma$ -bridge and  $\beta$ -nonbridge positions (lower part of Scheme VI). Contaminating  $P_i$  was present, allowing step 25 of the overall reaction to occur accounting for this result. In additional experiments, the PIX rate of both partial Reactions 24 and 25 are enhanced by phosphate. This is in accord with a mechanism in which phosphate adds prior to the first partial Reaction 24.

To test whether the second partial reaction occurs without added phosphate,  $\gamma^{18}\text{O}$ -ATP (I) was used.



Scheme VII

$^{18}\text{O}$  was found in the  $\beta$ -nonbridge position (ATP III) in an experiment started with ATP I and  $P_i$ . In addition, rotation around the central oxygen atom of pyrophosphate (IV) and backreaction to ATP should yield  $^{18}\text{O}$ -ATP V and this was found. In this reaction, one, two, or all terminal  $^{18}\text{O}$  atoms of ATP I can be exchanged for  $^{16}\text{O}$ . One  $^{18}\text{O}$  remains always attached to the  $\beta$ -P atom, either in a nonbridge or in the  $\beta\gamma$ -bridge position. In the same way,  $^{18}\text{O}$ ,  $^{18}\text{O}_2$ , and  $^{18}\text{O}_3$  phosphate is formed. All these different labeled phosphates and ATPs were detected in the  $^{31}\text{P}$ -NMR spectrum.<sup>37</sup>



Scheme VIII

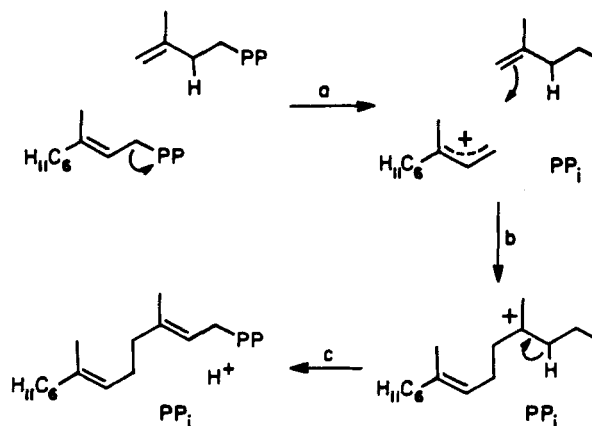
The experiments described above have provided new methods with which to probe the mechanism of this complicated multistep enzymatic mechanism.<sup>38</sup>

### B. Enzymes That Do Not Catalyze a PIX Reaction

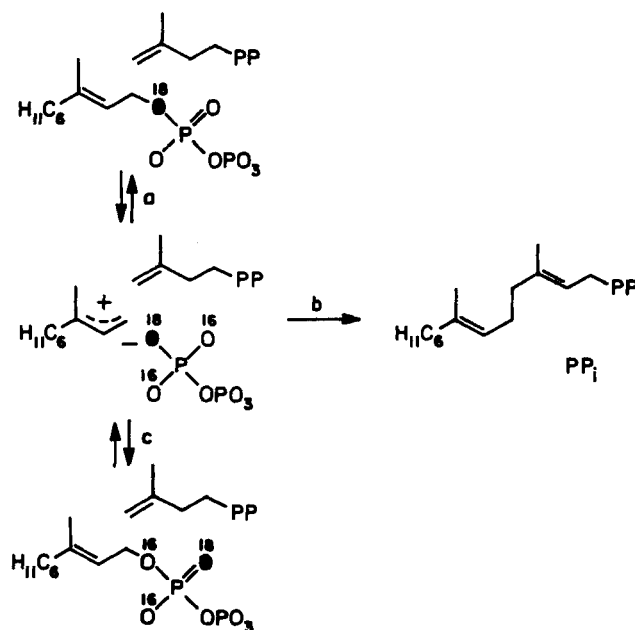
As outlined in the introduction there are a variety of conditions whereby a PIX reaction can be suppressed in an enzyme-catalyzed reaction even though an intermediate is formed and is capable of the positional exchange of the isotopes. The most insidious of these potential problems is restricted bond rotation. For a number of enzyme-catalyzed reactions this condition has already been documented.

#### 1. Farnesylpyrophosphate Synthetase

Farnesylpyrophosphate synthetase catalyzes the condensation between isopentenyl-PP and geranyl-PP as shown below:



Poulter et al.<sup>39</sup> have shown that the resonance-stabilized carbocation formed by the loss of PP<sub>i</sub> from geranyl-PP is an intermediate in this reaction. This was demonstrated by the large rate reductions caused by multiple fluorine substitution at the methyl group at C-3 of geranyl-PP. To confirm this proposal, Mash et al.<sup>40</sup> synthesized geranyl-PP labeled with <sup>18</sup>O as indicated below:

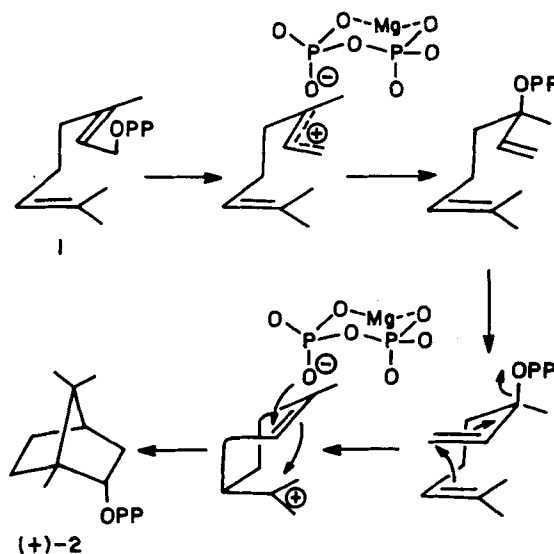




If a carbocation was formed then scrambling could occur within the  $PP_i$ . This would result in an  $^{18}O$  becoming incorporated into the nonbridging position in the geraniol after hydrolysis of the pyrophosphate. However, no scrambling could be detected even in the presence of isopentenyl-PP. It has thus been concluded that the intermediate must be a rigid geranyl cation-pyrophosphate anion pair that is unable to rotate at a significant rate.

## 2. Bornyl Pyrophosphate Synthetase

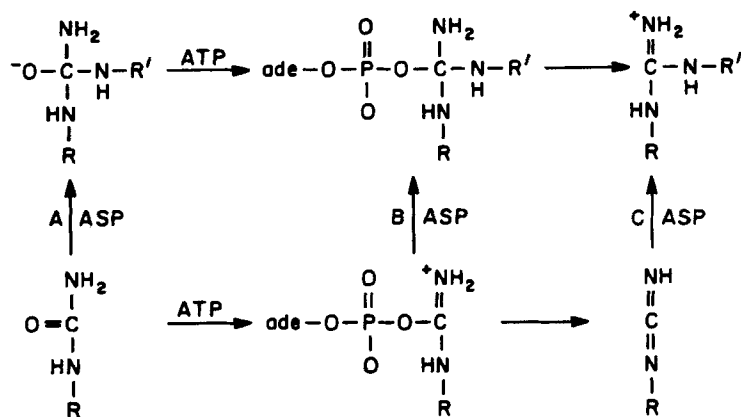
In a related example, Croteau et al.<sup>41</sup> examined the cyclization of geranyl pyrophosphate to bornyl pyrophosphate catalyzed by an enzyme from sage. The proposed mechanism for this transformation is illustrated below.



This mechanism requires two pyrophosphate migration steps in the formation of (+)-bornyl pyrophosphate. Croteau et al.<sup>41</sup> synthesized geranyl pyrophosphate labeled at C-1 with  $^{18}O$ . Incubation of the labeled geranyl pyrophosphate with enzyme resulted in the formation of bornyl pyrophosphate. After hydrolysis of the pyrophosphate moiety, MS demonstrated that the borneol possess an  $^{18}O$  enrichment identical with the acyclic precursor. Thus, in the transformation from geranyl pyrophosphate to bornyl pyrophosphate the C-O bond to the pyrophosphate moiety must be broken and reformed at an adjacent carbon center. Quite surprisingly, these results demonstrate that no PIX has occurred and thus the transformation from substrate to product must occur with remarkably tight restriction on the motion of the transiently generated pyrophosphate anion.

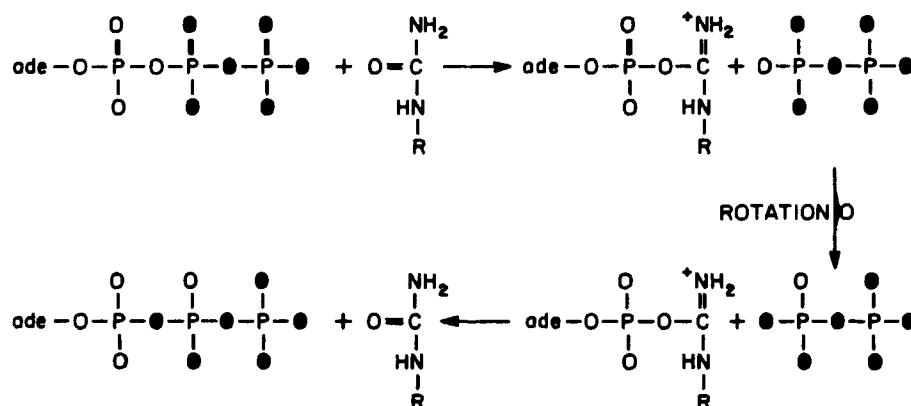
## 3. Argininosuccinate Synthetase

The enzyme argininosuccinate synthetase catalyzes the formation of argininosuccinate from ATP, citrulline, and aspartate. In a formal sense the reaction is quite similar to the reaction catalyzed by adenylosuccinate synthetase (see above). The primary difference being the use of adenylation rather than phosphorylation in the activation of the carbonyl oxygen. Three mechanisms have been proposed for this reaction as illustrated in Scheme IX below.



Scheme IX

Hilscher et al.<sup>13</sup> used PIX experiments to help in the distinction among these three mechanisms. If the citrulline is adenylylated prior to the attack by the aspartate then citrulline-adenylate would be a competent intermediate. Therefore, a PIX reaction should be observed as illustrated in Scheme X below.



Scheme X

However, no PIX could be observed under any reaction conditions when aspartate was omitted from the incubation mixture. This would suggest that either citrulline-adenylate is not formed before aspartate binds to the enzyme or there is restricted bond rotation about the P-O bond of pyrophosphate. In a subsequent paper, Ghose and Raushel<sup>42</sup> were able to demonstrate by rapid quench experiments that citrulline-adenylate was indeed formed. Furthermore, the rates of formation and equilibrium constants were also measured. The rate of formation is such that PIX should have readily occurred under the conditions employed by Hilscher et al.<sup>13</sup> Therefore, it must be concluded that the rotation of the phosphoryl group of the intermediate pyrophosphate must be restricted. This could occur by the complexation of the oxygen anions by  $Mg^{2+}$  and/or protein side chains.

#### 4. DNA Polymerase

DNA polymerase I catalyzes the template-directed synthesis of DNA from the various dNTPs. The reaction involves the attack of the 3'-hydroxyl of the growing DNA chain at

the  $\alpha$ -P of the dNTP. In an attempt to probe for the rate-limiting steps in this reaction, Mizrahi et al.<sup>43</sup> used  $[\alpha, \alpha\text{-}^{18}\text{O}_2]\text{dATP}$  to probe for an  $\alpha\beta$ -bridge to  $\beta$ -nonbridge isotope-exchange reaction during the template directed polymerization reaction. The existence of such an exchange would provide information on the partitioning of the E-PP<sub>i</sub>-primer complex. No exchange was observed. These observations are consistent with a model in which the rate of release of PP<sub>i</sub> from the E-PP<sub>i</sub>-primer complex is much faster than the rate of resynthesis and dissociation of the isotopically labeled dNTP from PP<sub>i</sub> and primer.

## REFERENCES

1. Rose, I. A., Positional isotope exchange studies of enzyme mechanisms, *Adv. Enzymol.*, 50, 361, 1979.
2. Wimmer, M. J., Rose, I. A., Powers, S. G., and Meister, A., Evidence that carboxyphosphate is a kinetically competent intermediate in the carbamyl phosphate synthetase reaction, *J. Biol. Chem.*, 254, 1854, 1979.
- 2a. Raushel, R. M. and Villafranca, J. J., Phosphorus-31 nuclear magnetic resonance application to positional exchange reactions catalyzed by *Escherichia coli* carbamoyl-phosphate synthetase: analysis of forward and reverse enzymatic reaction, *Biochemistry*, 19, 3170, 1980.
3. Midelfort, C. G. and Rose, I. A., A stereochemical method for detection of ATP terminal phosphate transfer in enzymatic reactions, *J. Biol. Chem.*, 251, 5881, 1976.
4. Rose, I. A., O'Connell, E. L., Litwin, S., and Bar-Tana, J., Determination of the rate of hexokinase-glucose dissociation by the isotope-trapping method, *J. Biol. Chem.*, 249, 5163, 1974.
5. Litwin, S. and Wimmer, M. J., Correction of scrambling rate calculation for loss of substrate, *J. Biol. Chem.*, 254, 1859, 1979.
6. Raushel, F. M. and Garrard, L. J., A positional isotope exchange study of the argininosuccinate lyase reaction, *Biochemistry*, 23, 1791, 1984.
7. Kenyon, G. L. and Reddick, R. E., NMR studies on  $^{15}\text{N}$ -labelled creatine, creatinine, phosphocreatine, and phosphocreatinine, and on barriers to rotation in creatine kinase-bound creatine in the enzymatic reaction, *Fed. Proc.*, 45, 1751, 1986.
8. Cleland, W. W., Partition analysis and the concept of net rate constants as tools in enzyme kinetics, *Biochemistry*, 14, 3220, 1975.
9. Raushel, F. M., Anderson, P. M., and Villafranca, J. J., Kinetic mechanism of *Escherichia coli* carbamoyl-phosphate synthetase, *Biochemistry*, 17, 5587, 1978.
10. Hester, L., Hilscher, L., and Raushel, F. M., A positional isotope exchange analysis of the uridine-diphosphoglucose reaction, *Fed. Proc.*, 45, 1914, 1986.
11. Tsuboi, K. K., Fukunaga, K., and Petricciani, J. C., Purification and specific kinetic properties of erythrocyte uridine diphosphate glucose pyrophosphorylase, *J. Biol. Chem.*, 244, 1008, 1969.
12. Webb, M. R., A method for determining the positional isotope exchange in a nucleoside triphosphate: cyclization of nucleoside triphosphate by dicyclohexylcarbodiimide, *Biochemistry*, 19, 4744, 1980.
13. Hilscher, L. W., Hanson, C. D., Russell, D. H., and Raushel, F. M., Measurement of positional isotope exchange rates in enzyme-catalyzed reactions by fast atom bombardment mass spectrometry: application to argininosuccinate synthetase, *Biochemistry*, 24, 5888, 1985.
14. Cohn, M. and Hu, A., Nuclear magnetic resonance applied to a study of enzyme catalyzed phosphate-phosphate exchange and phosphate (oxygen)-water exchange reactions, *Proc. Natl. Acad. Sci. U.S.A.*, 75, 200, 1978.
15. Reynolds, M. A., Oppenheimer, N. J., and Kenyon, G. L., Enzyme-catalyzed positional isotope exchange by phosphorus-31 nuclear magnetic resonance spectroscopy using either  $^{18}\text{O}$ - or  $^{18}\text{O}$ - $\beta$ , $\gamma$ -bridge-labelled adenosine 5'-triphosphate, *J. Am. Chem. Soc.*, 105, 6663, 1983.
16. Tsai, M. D., Use of phosphorus-31 nuclear magnetic resonance to distinguish bridge and nonbridge oxygen of oxygen-17 enriched nucleoside triphosphate, *Biochemistry*, 18, 1468, 1979.
17. Anderson, P. M. and Meister, A., Bicarbonate-dependent cleavage of adenosine triphosphate and other reactions catalyzed by *Escherichia coli* carbamyl phosphate synthetase, *Biochemistry*, 5, 3157, 1966.
18. Lowe, G. and Sproat, B., Evidence for a dissociate S<sub>N</sub>1(P) mechanism of phosphoryl transfer by rabbit muscle pyruvate kinase, *J. Chem. Soc. Perkin Trans.*, 1622, 1979.
19. Hassett, A., Blattler, W., and Knowles, J. R., Pyruvate kinase: is the mechanism of phospho transfer associative or dissociative?, *Biochemistry*, 21, 6335, 1982.
20. Lowe, G. and Sproat, B. S., Evidence for an associative mechanism in the phosphoryl transfer step catalyzed by rabbit muscle creatine kinase, *J. Biol. Chem.*, 255, 3944, 1980.

21. Rose, I. A., Mechanism of phosphoryl transfer by hexokinase, *Biochem. Biophys. Res. Commun.*, 94, 573, 1980.
22. Bass, M. B., Fromm, H. F., and Rudolf, F. B., The mechanism of the adenylosuccinate synthetase reaction as studied by positional isotope exchange, *J. Biol. Chem.*, 259, 12330, 1984.
23. Baldwin, A. N. and Berg, P., Transfer ribonucleic acid-induced hydrolysis of valyladenylate bound to isoleucyl ribonucleic acid synthetase, *J. Biol. Chem.*, 241, 839, 1966.
24. Kisselev, L. L. and Favorova, O. O., Aminoacyl-tRNA synthetases: some recent results and achievements, *Adv. Enzymol.*, 40, 141, 1974.
25. Smith, L. T. and Cohn, M., Role of the  $\beta$ -phosphate- $\gamma$ -phosphate interchange reaction of adenosine triphosphate in amino acid discrimination by valyl- and methionyl-tRNA synthetases from *Escherichia coli*, *Biochemistry*, 20, 385, 1981.
26. Lowe, G., Sproat, B. S., Tansley, G., and Cullis, P. M., A stereochemical and positional isotope exchange study of the mechanism of activation of isoleucine by isoleucyl-tRNA synthetase from *Escherichia coli*, *Biochemistry*, 22, 1229, 1983.
27. Lowe, G., Sproat, B. S., and Tansley, G., A stereochemical and positional isotope-exchange study of the mechanism of activation of methionine by methionyl-tRNA synthetase from *Escherichia coli*, *Eur. J. Biochem.*, 130, 341, 1983.
28. Lowe, G. and Tansley, G., A stereochemical and positional isotope exchange study of the mechanism of activation of tyrosine by tyrosyl-tRNA synthetase from *Bacillus stearothermophilus*, *Tetrahedron*, 40, 113, 1984.
29. Meek, T. D., Johnson, K. A., and Villafranca, J. J., *E. coli* glutamine synthetase: determination of rate-limiting steps by rapid-quench and isotope partitioning experiments, *Biochemistry*, 21, 2158, 1982.
30. Stokes, B. O. and Boyer, P. D., Rapid transfer of oxygens from inorganic phosphate to glutamine catalyzed by *Escherichia coli* glutamine synthetase, *J. Biol. Chem.*, 251, 5558, 1976.
- 30a. Clark, D. D. and Villafranca, J. J., Isotope-exchange enhancement studies of *E. coli* glutamine synthetase, *Biochemistry*, 24, 5147, 1985.
31. Meek, T. D. and Villafranca, J. J., Kinetic mechanism of *E. coli* glutamine synthetase, *Biochemistry*, 19, 5513, 1980.
32. Wedler, F. C. and Boyer, P. D., Substrate binding and reaction intermediates of glutamine synthetase (*E. coli* w) as studied by isotope exchange, *J. Biol. Chem.*, 247, 984, 1972.
33. Levitski, A. and Koshland, D. E., Jr., Cytidine triphosphate synthetase. Covalent intermediates and mechanism of action, *Biochemistry*, 10, 3365, 1971.
34. von der Saal, W., Anderson, P. M., and Villafranca, J. J., Mechanistic investigations of *Escherichia coli* cytidine-5'-triphosphate synthetase, *J. Biol. Chem.*, 260, 14993, 1985.
35. von der Saal, W., Crysler, C. S., and Villafranca, J. J., Positional isotope exchange and kinetic experiments with *Escherichia coli* guanosine-5'-monophosphate synthetase, *Biochemistry*, 24, 5343, 1985.
36. Wang, H.-C., Ciskanik, L., Dunaway-Mariano, D., von der Saal, W., and Villafranca, J. J., Investigations of the partial reactions catalyzed by pyruvate phosphate dikinase, *Biochemistry*, in press.
37. von der Saal, W. and Villafranca, J. J.,  $^{18}\text{O}$  isotope shift effect in the  $^{31}\text{P}$ -NMR spectra of the terminal phosphate groups of ADP and ATP: a reinvestigation, *Bioorg. Chem.*, 14, 28, 1986.
38. Milner, Y., Michaels, G., and Wood, H. G., Pyruvate, phosphate dikinase of *Bacteroides symbiosus*. Catalysis of partial reactions and formation of phosphoryl and pyrophosphoryl forms of the enzyme, *J. Biol. Chem.*, 253, 878, 1978.
39. Poulter, C. D., Wiggins, P. L., and Le, A. T., Farnesylpyrophosphate synthetase. A stepwise mechanism for the 1'-4 condensation reaction, *J. Am. Chem. Soc.*, 103, 3926, 1981.
40. Mash, E. A., Gurria, G. M., and Poulter, C. D., Farnesylpyrophosphate synthetase. Evidence for rigid geranyl cation-pyrophosphate anion pair, *J. Am. Chem. Soc.*, 103, 3927, 1981.
41. Croteau, R. B., Shaskeu, J. J., Renstrom, B., Felton, N. M., Cane, D. E., Saito, A., and Chang, C., Mechanism of the pyrophosphate migration in the enzymatic cyclization of geranyl and linalyl pyrophosphate to (+)- and (-)-bornyl pyrophosphates, *Biochemistry*, 24, 7077, 1985.
42. Ghose, C. and Raushel, F. M., Determination of the mechanism of the argininosuccinate synthetase reaction by static and dynamic quench experiments, *Biochemistry*, 24, 5894, 1985.
43. Mizrahi, V., Henrie, R. N., Marlier, J. F., Johnson, K. A., and Benkovic, S. J., Rate-limiting steps in the DNA polymerase I reaction pathway, *Biochemistry*, 24, 4010, 1985.